University of Thi-Qar Journal for Engineering Sciences
http://www.doi.org/10.31663/tqujes.12.1.404(2022)
Vol 12.1(April2022)

ISSN :2664- 5572 (online)
ISSN:2664-5564 (print)
Available at http://jeng.utq.edu.iq
utjeng@ utq.edu.iq

Enhancing Heat Transfer Using Multi-Size Teardrops obstacles

Mohsen H. Fagr[†], Hayder M. Hasan[‡] and Zaher M. A. Alsulaiei[†]
† Mech. Eng. Dept. University of Thi-qar, Nasseriya, Iraq, mohafagr@yahoo.com & mohsenfagr@ utq.edu.iq.
‡ Thi qar Technical College, Southern Technical University, Nasseriya, Iraq, hayder.mohammad@stu.edu.iq.
† Biomedical Eng. Dept. University of Thi-qar, Nasseriya, Iraq, Zaheralsulaiei@utq.edu.iq.

Abstract

In this paper, heat transfer enhancements using unique, various sets of teardrop-shapes inserts in a heating tube are numerically examined. The teardrop is a hemispheric placed on a conic part. The three-dimensional continuity, momentum and energy equations are repeatedly solved using ANSYS 17.1 software at turbulent flow regime with Reynolds number varies from 10000 to 30000. Nine cases are investigated excluding the plain tube case by changing the ratios of hemisphere diameter and conic part length to the tube diameter, dr and lr respectively. The tube was of diameter and length of 30 mm and 1000 mm respectively. The tested ratios were dr = 1/3, 1/2 and 2/3 while the ratio lr =5/3, 7.5/3 and 10/3. The results show that Nusselt number increases with increasing both dr and lr and vice versa because the greater dr interrupts the flow and therefore boosts swirling power in the tube. Similarly, the friction factor behaves as a consequence of the large blockage presence. However, the thermal performance factor *TPF* is less at the greatest dr and lr ratios, and the optimal one is obtained when the equipped teardrops were of dr=2/3 and lr=5/3 recording *TPF*=1.32 which is the most thermally efficient case among the rest. Over the empty tube, the percentage increase in *TPF* is 32% and 11% at Re=10000 and Re=30000 respectively. While the percentages in comparison with the smallest dr and lr are 11.8% at Re=10000 and 4.7% at Re=30000.

Keywords: teardrop obstacles, thermal performance factor.

1. Introduction

Enhancing heat transfer in the heat exchangers is a continuous operation due to the continuous increase in our demands for power in all devices that promote modernity in our life. Nuclear reactors, power generating, food and chemical processing, industrial and medical devices are some examples of the devices that have heat exchangers. The used techniques for enhancing heat transfer can be classified into; active, passive and compound **[1-3]**. Active techniques need additional external power, while passive techniques do not have this needing which gave them good research attention. Therefore, more and more scientific efforts were concerned with passive techniques for enhancing heat transfer in heat exchangers. Techniques of turbulence promotors are widely used to achieve this goal. Corrugated surfaces were studied **[4-8]** to show the effects of these surfaces on heat transfer. Effects of inserting many models of twisted tapes on heat transfer in heat exchangers have very good scientific consideration **[9-13]**. Many researchers studied heat transfer enhancements through using sudden expansion channels, plain or equipped by obstacles **[14-18]**. Also, the effects of roughened surfaces on natural and forced convective heat transfer were investigated **[19-21]**. For increasing flow paths and rotational flow pattern, twisted tubes of different cross-sections were studied and good results were achieved **[22-26]**. Fagr et. al. **[27]** revealed good numerical results in enhancing heat transfer in a tube through using helical obstacle.

Teardrops, or streamline shapes, turbulence promoters were used firstly by Lawrence B. Evans through his PhD thesis in 1962 **[28]**, his teardrops were made of nylon due to the low manufacturing cost comparing to the metallic inserts, lightweight and corrosion resistance. Since this year, Evans experimental effort was the unique effort that studied the use of teardrops for generating swirling force to the flow and hence enhancing heat transfer. So, the present paper reintroduces these turbulence promoters by studying the effects of the insertion of three teardrops in a tube on heat transfer and flow fields. Here, we consider the simultaneous effects of both hemisphere diameter ratio dr (divided by the tube diameter for generality), and conic shape length ratio lr (also generalized with the tube diameter). Moreover, the flow direction is opposed here to face the end of the conic shape and then propagates gradually to reach the hemispheric part at the end of the teardrop along with a new numerical procedure and higher flow intensity than studied before (Reynolds number of $10000 \leq Re \leq 30000$). The proposal study deals with nine

cases of various teardrops shapes which are compared to each other and with the empty tube revealing the optimal thermal and hydraulic performance for all cases; this will be detailed in the next sections.

2. Problem sets

The configuration of teardrop-like inserts in a heating tube is shown in **Fig.1** which consists of a cone of length (l) connected in its base and top with hemispheres of diameters (d1) and (d2) respectively.

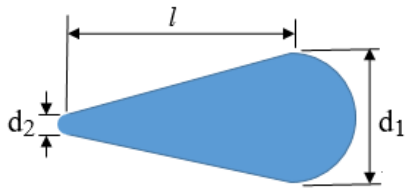

Fig. 1 Schematic diagram for a teardrop.

The teardrops are placed along the tube length as detailed in Fig.2. The figure represents a schematic diagram of a circular tube fitted with obstacles of teardrop-like shape. The horizontal tube has a surface of negligible thickness and it is 30 mm diameter (D) and 1000 mm length (L).

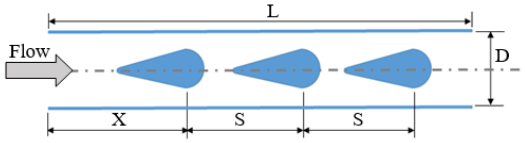

Fig. 2 Schematic diagram of a tube equipped with three teardrops-like inserts.

Three identical teardrops are used, and they are installed at the centerline of the tube. The first one has a distance (X) from the tube inlet and there is a space between every two obstacles (S). X and S were 200 mm and 150 mm respectively. The tested teardrop lengths (l) are 50 mm, 75 mm and 100 mm giving the length ratio (lr = l/D) of 5/3, 7.5/3 and 10/3 respectively. The large hemisphere diameter (d1) is 10 mm, 15 mm and 20 mm giving diameter ratios (dr = d1/ D) of 1/3, 1/2 and 2/3 respectively. Hence, nine cases shall be investigated excluded the plain tube where at every d1 value the teardrop length ratio will be replaced with corresponding values.

3. Governing equations

In the presented problem, the flow is assumed as a steady-state, three dimensional and turbulent flow regime (Reynolds number of $10000 \leq Re \leq 30000$. The mass and momentum conservation equations are prescribed mathematically through continuity and momentum equations. Also, the energy equation is required. Those governing equations are **[29]**:

Continuity equation

$$\frac{\partial \bar{u}}{\partial x} + \frac{\partial \bar{v}}{\partial y} + \frac{\partial \bar{w}}{\partial z} = 0 \quad \textbf{(1)}$$

X-direction momentum equation;

$$\left(\bar{u}\frac{\partial \bar{u}}{\partial x} + \bar{v}\frac{\partial \bar{u}}{\partial y} + \bar{w}\frac{\partial \bar{u}}{\partial z}\right) + \left(\frac{\partial}{\partial x}\overline{(u'^2)} + \frac{\partial}{\partial y}\overline{(u'v')} + \frac{\partial}{\partial z}\overline{(u'w')}\right) = -\frac{1}{\rho}\frac{\partial p}{\partial x} + \upsilon \nabla^2 \bar{u} \quad \textbf{(2)}$$

Y-direction momentum equation;

$$\left(\bar{u}\frac{\partial \bar{v}}{\partial x} + \bar{v}\frac{\partial \bar{v}}{\partial y} + \bar{w}\frac{\partial \bar{v}}{\partial z}\right) + \left(\frac{\partial}{\partial x}\overline{(u'v')} + \frac{\partial}{\partial y}\overline{(v'^2)} + \frac{\partial}{\partial z}\overline{(v'w')}\right) = -\frac{1}{\rho}\frac{\partial p}{\partial y} + \upsilon \nabla^2 \bar{v} \quad \textbf{(3)}$$

Z-direction momentum equation;

$$\left(\bar{u}\frac{\partial \bar{w}}{\partial x} + \bar{v}\frac{\partial \bar{w}}{\partial y} + \bar{w}\frac{\partial \bar{w}}{\partial z}\right) + \left(\frac{\partial}{\partial x}\overline{(u'w')} + \frac{\partial}{\partial y}\overline{(v'w')} + \frac{\partial}{\partial z}\overline{(w'^2)}\right) = -\frac{1}{\rho}\frac{\partial p}{\partial z} + \upsilon \nabla^2 \bar{w} \quad \textbf{(4)}$$

Energy equation;

$$\bar{u}\frac{\partial \bar{T}}{\partial x} + \bar{v}\frac{\partial \bar{T}}{\partial y} + \bar{w}\frac{\partial \bar{T}}{\partial z} = \alpha \nabla^2 \bar{T} - \left(\frac{\partial}{\partial x}\overline{(u'T')} + \frac{\partial}{\partial y}\overline{(v'T')} + \frac{\partial}{\partial z}\overline{(w'T')}\right) \quad \textbf{(5)}$$

ANSYS 17.1 was used to predict the flow and heat transfer behavior. For simplifying, the momentum and energy equations were solved under some assumptions as: (1) the flow is steady, turbulent and incompressible. (2) body forces, thermal radiation and natural convection are neglected. (3) temperature-independent thermo-physical properties are selected for the fluid. The finite volume method was selected to discretize the partial forms of the governing equations. Also, the K-ε model was chosen. For the pressure field evaluation, the pressure–velocity coupling algorithm SIMPLE (Semi Implicit Method for Pressure-Linked Equations) was selected. 10^{-6} was used as convergence criteria for all variables.

Inlet Reynolds number was;

$$\mathrm{Re} = \frac{\rho\, u_{av.}\, D}{\mu} \quad \textbf{(6)}$$

Nusselt number will be calculated as:

$$Nu = \frac{h\, D}{k} \quad \textbf{(7)}$$

Where the average coefficient of convective heat transfer h will be:

$$h = \frac{q''}{T_s - T_b} \quad \textbf{(8)}$$

The average friction factor was calculated according to the equation below **[30]**:

$$f = \frac{\Delta P_t}{\frac{1}{2}\rho\, u_{av.}^2}\,\frac{D}{L} \quad \textbf{(9)}$$

Thermal performance factor TPF, proposed by Webb **[31]**, based on the tradeoff between increased heat transfer and friction factor, is defined as **[32]**:

$$TPF = \left(Nu / Nu_p\right)\left(f / f_p\right)^{-1/3} \quad \textbf{(10)}$$

4. Boundary Conditions

For the tube, its wall was selected as a stationary wall and was under constant heat flux (2000 W/m^2). Uniform velocity and constant temperature were selected for air at the tube inlet. Pressure outlet condition is used with zero pressure gage. Conduction heat transfer through the obstacles was neglected. The airflow was turbulent with Reynolds number of $10000 \leq Re \leq 30000$. The velocity and turbulent intensity were specified according to the Reynolds number.

5. Mesh generation and its independency

Unstructured mesh was used to divide the 3D domains in the present study due to the complexity of these flow domains. Moreover, tetrahedral elements of non-uniform type were selected due to their flexibility as seen in Fig. 3.

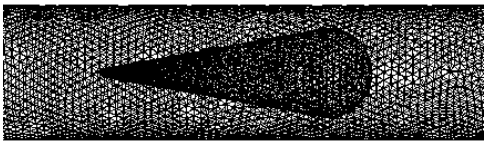

Fig. 3 Tetrahedral mesh of tube with teardrops of diameter and length ratios of 2/3 and 5/3 respectively.

To reach accurate results, the specified number of elements is very important to give independent results. So, for obtaining the stable results, refinement of mesh was tested. Figs. 4 and 5, for example, show Nusselt number and friction factor when the tube was equipped by teardrops of diameter and length ratios of 1/3 and 7.5/3 respectively under a different number of elements. As cleared in these figures, the second division has the stable results where the differences in the results were less than 1%.

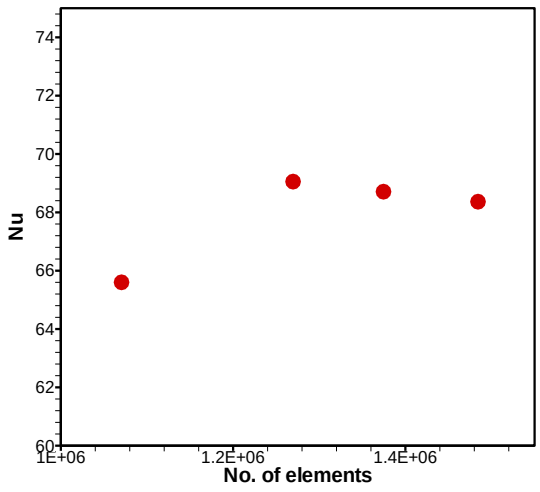

Fig. 4 Nusselt number for tube equipped by three teardrops of diameter and length ratios of 1/3 and 7.5/3 respectively at a different number of elements at Re = 20000.

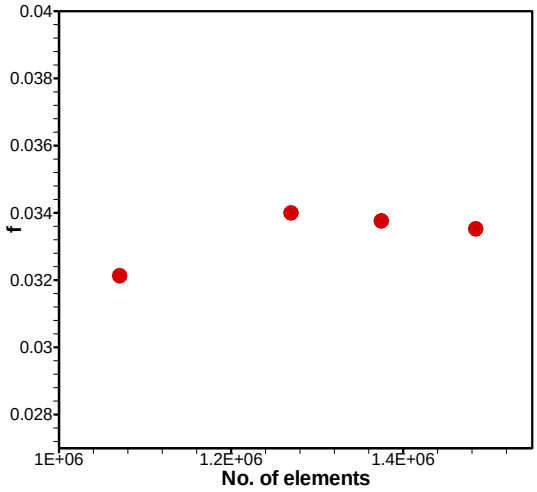

Fig. 5 friction factor for tube equipped by three teardrops of diameter and length ratios of 1/3 and 7.5/3 respectively at a different number of elements at Re = 20000.

According to the consideration of mesh independence, the used numbers of elements of the studied cases are shown in Table (1).

Table (1) The studied cases and their specified number of elements.

Case No.	teardrop ratios	No. of elements
1	dr = 1/3, lr = 5/3	1211554
2	dr = 1/3, lr = 7.5/3	1269600
3	dr = 1/3, lr = 10/3	1310972
4	dr = 1/2, lr = 5/3	1160089
5	dr = 1/2, lr = 7.5/3	1200417
6	dr = 1/2, lr = 10/3	1229227
7	dr = 2/3, lr = 5/3	1146107
8	dr = 2/3, lr = 7.5/3	1176710
9	dr = 2/3, lr = 10/3	1204215
10	Plain tube	631685

5. Comparisons with other studies

The numerical Nusselt number, as well as friction factor those obtained for plain tube in this work were compared with previous works. Nusselt number was compared with the correlation of Dittus-Boelter correlation **[30]**:

$$Nu = 0.023\ Re^{0.8}\ Pr^{0.4} \quad \textbf{(11)}$$

Also, the friction factor was compared with the correlation of Petukhov **[33]**:

$$f = (0.79\ \ln Re - 1.64)^{-2} \quad \textbf{(12)}$$

The results of these two comparisons are shown in Figs. 6 and 7 respectively.

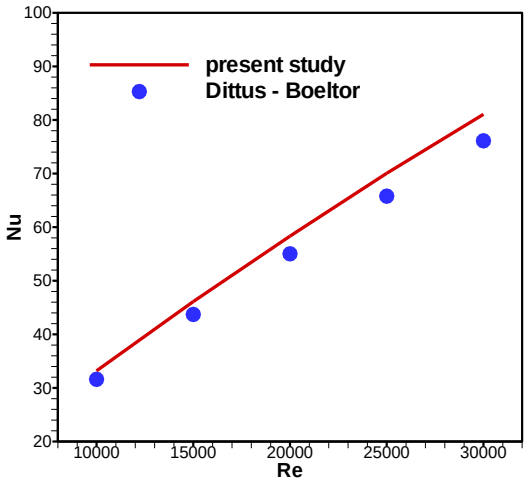

Fig. 6 Comparison of Nusselt number.

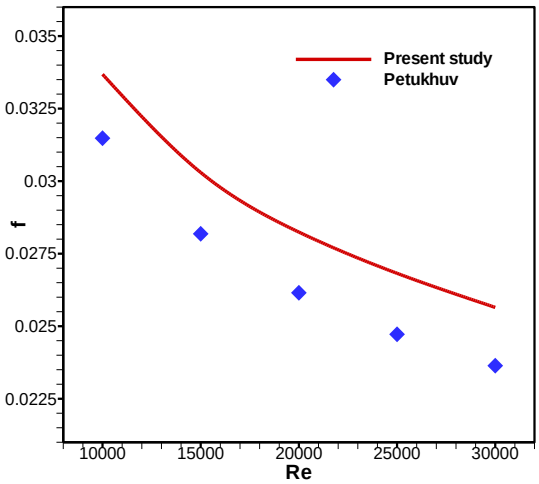

Fig. 7 Comparison of friction factor.

According to these two figures, there are good agreements for the results of the present work. The average deviations between Nusselt number of present work and Dittus-Boelter correlation and between the friction factor of the present work and the Petukhov correlation were 6 % and 8 % respectively.

6. Results and discussions

Three-dimensional fluid flow and heat transfer equations within the flow are solved with convenient boundary conditions in nine cases excluding the plain tube case. So, we will discuss the effect of the use of teardrops in a heating tube subjected to 2000 W/m2 of constant heat flux. The results are evaluated at every diameter ratio (dr=d1/D), there will be three corresponding findings given for three teardrop length ratios (lr=l/D). This is already detailed in Table 1 where D is the tube diameter (D=30 mm in all cases), d1 is the largest teardrop shape hemisphere diameter (d1=10, 15 and 20 mm), and l is the length of teardrop conic part (l=50, 75 and 100 mm).

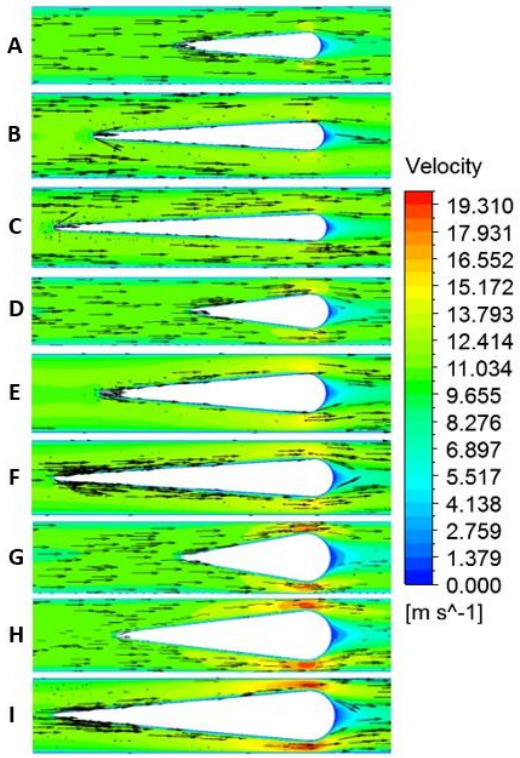

Fig. 8 Velocity vector and contour for tube equipped by three teardrops of different diameter and length ratios (A) dr=1/3 and lr=5/3, (B) dr=1/3 and lr=7.5/3, (C) dr=1/3 and lr=10/3, (D) dr=1/2 and lr=5/3, (E) dr=1/2 and lr=7.5/3, (F) dr=1/2 and lr=10/3, (G) dr=2/3 and lr=5/3, (H) dr=2/3 and lr=7.5/3 and (I) dr=2/3 and lr=10/3 for Re = 20000 at the second teardrop.

The revealed contours in **Figs. 8 and 9** for the velocity and temperature distributions for all cases considered. We can notice that the first three cases are plotted at the same dr=1/3 ratio (i.e. A, B and C), the second group is presented at dr=1/2 (D, E and F). The last group is given at dr=2/3 (F, G and H). In every single group, the ratio lr=l/D varies three times corresponding to the changing teardrop length. The higher dr ratio gives more swirling force to the fluid as illustrated in the last three cases in Fig. 8 where the fluid directed away from the tube center and comes close to the tube wall. As results, the higher heat transfer rates would be anticipated as plotted in Fig. 9 for the last three cases. The rest of the cases come after in terms of flow and temperature as results of smaller dr ratios. In other words, the largest dr ratio gives the greatest circulation force to the fluid and then enhances the heat transfer rate.

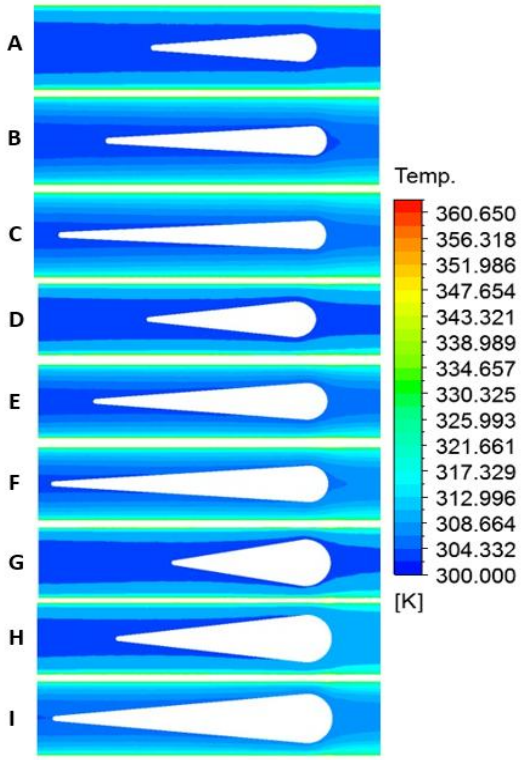

Fig. 9 Temperature contour for tube equipped by three teardrops of different diameter and length ratios (A) dr=1/3 and lr=5/3, (B) dr=1/3 and lr=7.5/3, (C) dr=1/3 and lr=10/3, (D) dr=1/2 and lr=5/3, (E) dr=1/2 and lr=7.5/3, (F) dr=1/2 and lr=10/3, (G) dr=2/3 and lr=5/3, (H) dr=2/3 and lr=7.5/3 and (I) dr=2/3 and lr=10/3 for Re = 20000 at the second teardrop.

The variations of Nusselt number with Re are detailed in Figs. 10 and 11 without and with normalizing respectively with the Nusselt number for the plain tube (i.e. Nu and Nu/Nup). The comparisons between all cases and with the plain tube demonstrate that the systematic increase in Nu with dr and lr where the optimal Nu observed at dr=2/3 and lr=10/3. The percentage rise in Nu number in this case compared to the empty tube is summarized in Table 2. The Table shows that the greater dr and lr case gives the higher Nu number (i.e. case 9). Therefore, the percentage increases in Nu numbers are 52% and 24% at Re=10000 and Re=30000 respectively over the plain tube. Whereas the percentage rise from the smallest dr and lr (case 1) to the last one (case 9) is 100% at Re=10000 and 118 % at Re=30000. This interesting boosts in thermal performance are appreciated in the heat exchangers industry.

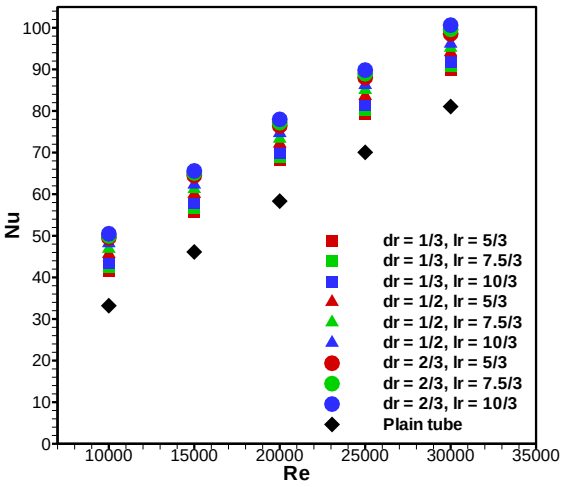

Fig. 10 Nusselt number variation with Reynolds number.

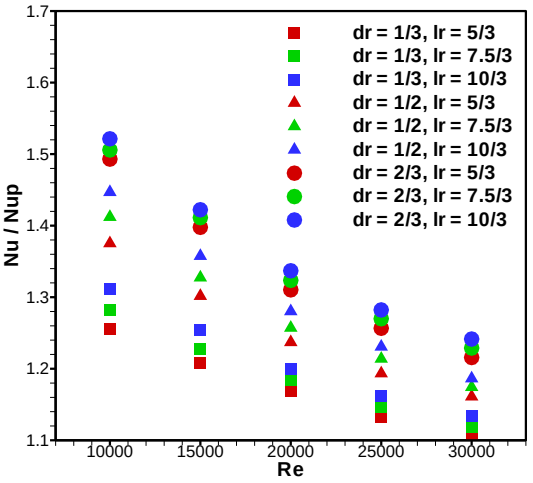

Fig. 11 Nusselt number ratio variation with Reynolds number.

Table (2) Increase in Nusselt number for the studied cases.

Case No.	Teardrop ratios	% increasing in Nu	
		From Re= 10000	To Re= 30000
1	dr = 1/3, lr = 5/3	26	11
2	dr = 1/3, lr = 7.5/3	28	12
3	dr = 1/3, lr = 10/3	31	13
4	dr = 1/2, lr = 5/3	36	16
5	dr = 1/2, lr = 7.5/3	41	17
6	dr = 1/2, lr =	45	19

	10/3		
7	dr = 2/3, lr = 5/3	49	22
8	dr = 2/3, lr = 7.5/3	51	23
9	dr = 2/3, lr = 10/3	52	24

The higher friction losses penalties are associated with the greater Nu number discussed previously. So, **Figs. 12 and 13** prove these behaviors showing that the greater dr and lr ratios generate the highest friction factors in comparison to each other or with the plain tube (i.e. f /fp). This an understandable tend as the dr is increasing the teardrop body interrupts more the flow motion, also the longest teardrop tail, thus friction rises. The results are reflected in Table 3, where the percentage increases in friction factors (case 9) are 59% and 41% at Re=10000 and Re=30000 respectively over the plain tube. Whereas the percentage rises from the smallest dr and lr (case 1) to the last case 9 are 195% and 173.3 % at Re=10000 and Re=30000 respectively.

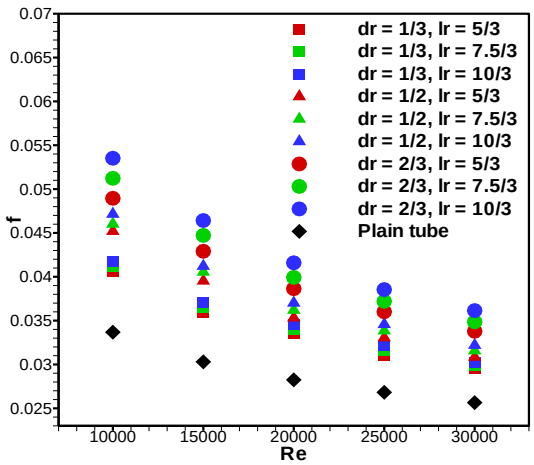

Fig. 12 friction factor variation Reynolds number.

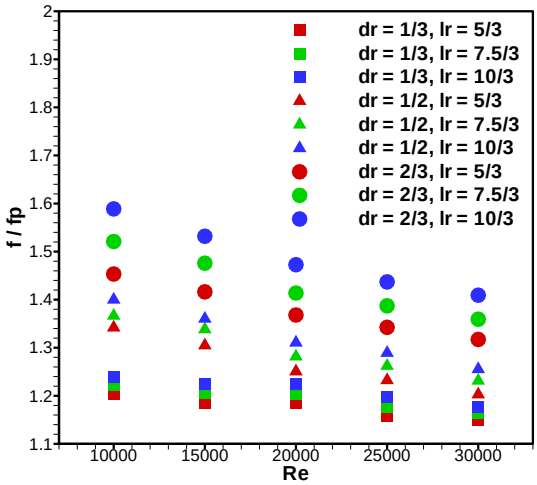

Fig. 13 friction factor ratio variation with Reynolds number.

Table (3) Increase in friction factor for the studied cases.

Case No.	Teardrop ratios	% increasing in f	
		From Re= 10000	To Re= 30000
1	dr = 1/3, lr = 5/3	20	15
2	dr = 1/3, lr = 7.5/3	22	16
3	dr = 1/3, lr = 10/3	24	18
4	dr = 1/2, lr = 5/3	34	20
5	dr = 1/2, lr = 7.5/3	37	23
6	dr = 1/2, lr = 10/3	40	26
7	dr = 2/3, lr = 5/3	45	32
8	dr = 2/3, lr = 7.5/3	52	36
9	dr = 2/3, lr = 10/3	59	41

The convenient thermal performance factor TPF is plotted against the Reynolds number in **Fig. 14** and reflected in **Table 4** for all cases. TPF is beyond unity for all cases which refers to that the heat transfer rate has increased. The figure shows that the greater teardrop length lr=10/3 ratio does not produce the higher TPF especially at Re=10000 because the longest tail generates more friction force. While the shortest teardrop with the higher dr gives the optimal performance (i.e. dr=2/3 and lr=5/3 case). At higher Re, all cases tend to gather closer because the flow is predominated by flow velocity making the insertion effect is less. Thus, the table indicates that case 7 is the most efficient one among the rest for Re ranges considered in this study. Using longer teardrop (cases 8 and 9) does not enhance heat transfer more than case 7. The overall thermal performance factor increase from case 1 to 7 is 11.8% at Re=10000, while at Re=30000 the percentage rise is 4.7%.

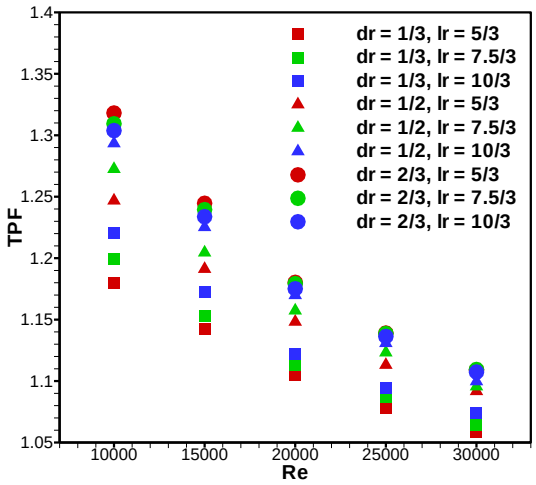

Fig. 14 thermal performance factor variation with Reynolds number.

Table 4 thermal performance factor for the studied cases.

Case No.	Teardrop ratios	TPF	
		From Re= 10000	To Re= 30000
1	dr = 1/3, lr = 5/3	1.18	1.06
2	dr = 1/3, lr = 7.5/3	1.2	1.06
3	dr = 1/3, lr = 10/3	1.22	1.07
4	dr = 1/2, lr = 5/3	1.25	1.1
5	dr = 1/2, lr = 7.5/3	1.27	1.1
6	dr = 1/2, lr = 10/3	1.29	1.1
7	dr = 2/3, lr = 5/3	1.32	1.11
8	dr = 2/3, lr = 7.5/3	1.31	1.11
9	dr = 2/3, lr = 10/3	1.3	1.11

Conclusion

Three-dimensional continuity, momentum and energy equations have been solved using ANSYS 17.1 software at turbulent flow conditions (Reynolds number ranges from 10000 to 30000). Nine cases have been examined excluding the empty tube case by varying ratios dr and lr (hemisphere to the tube diameters ratio and conic shape length to the tube diameter ratio respectively) in a tube of a fixed diameter and length and exposed to constant heat flux. The effects of the three identical inserted teardrops on both thermal and hydraulic performance have been analyzed through various comparisons between the new cases and the plain tube, and between each other. Thus, the following concluding remarks can be drawn:

1. Teardrop-like shapes inserts can be used to stimulate the swirling power to flow efficiently as similar to any other common inserts.
2. The anticipated behaviours of both Nusselt number and friction factor have been also observed here, where both increase with dr and lr ratios and vice versa.
3. Thermal performance factor TPF is more than 1 for all nine cases considered.
4. The optimal TPF has been noticed at the largest dr and smallest lr ratios which reaches 1.32 at Re=10000 and 1.11 at Re=30000. This generates an increase of 32% and 11% over the empty tube.

References

[1] C. Maradiya, J. Vadher, R. Agarwal, The heat transfer enhancement techniques and their Thermal Performance Factor, *Beni-Suef University Journal of Basic and Applied Sciences*, 2018,7,1.

[2] N. A. C. Sidik, M. N. A. W. Muhamad, W. M. A. A. Japar, Z. A. Rasid, An overview of passive techniques for heat transfer augmentation in microchannel heat sink, International Communications in Heat and Mass Transfer, 2017.

[3] R. Gugulothu, K. V. K. Reddy, N. S. Somanchi, E. L. Adithya, A Review on Enhancement of Heat Transfer Techniques, Materialstoday: Proceedings 2017,4,1051.

[4] A. Begag, R. Saim, S. Abboudi, H. F.Öztop, Effect of internal and external corrugated surfaces on the characteristics of heat transfer and pressure drop in a concentric tube heat exchanger, *International Journal of Thermal Sciences*, 2021,165,106930.

[5] A. Mazhar, S. Liu, A. Shukla, Numerical investigation of the heat transfer enhancement using corrugated pipes in a PCM for grey water harnessing, Thermal Science and Engineering Progress, 23 (2021) 100909.

[6] V. Q. Hoang, T. T. Hoang, C. T. Dinh, F. Plourde, Large eddy simulation of the turbulence heat and mass transfer of pulsating flow in a V-sharp corrugated channel, *International Journal of Heat and Mass Transfer*, 2021,166,120720.

[7] J. I. Córcoles, J. D. Moya-Rico, A. E. Molina, J. A. Almendros-Ibáñez, Numerical and experimental study of the heat transfer process in a double pipe heat exchanger with inner corrugated tubes, *International Journal of Thermal Sciences*, 2020,158,106526.

[8] F. Andrade, A. S. Moita, A. Nikulin, A. L. N. Moreira, H. Santos, Experimental investigation on heat transfer and pressure drop of internal flow in corrugated tubes, *International Journal of Heat and Mass Transfer*, 2019,140,940-955.
[9] M. H. Fagr, Q. A. Rishak, K. S. Mushatet, Performance evaluation of the characteristics of flow and heat transfer in a tube equipped with twisted tapes of new configurations, *International Journal of Thermal Sciences* 2020,153,106323.
[10] K. S. Mushatet, Q. A. Rishak, M. H. Fagr, Experimental and Numerical Investigation of Swirling Turbulent Flow and Heat Transfer Due To Insertion of Twisted Tapes of New models in a Heated Tube, Applied Thermal Engineering 2020,171,115070.
[11] V. Singh, S. Chamoli, M. Kumar, A. Kumar, Heat transfer and fluid flow characteristics of heat exchanger tube with multiple twisted tapes and solid rings inserts, Chemical Engineering and Processing 2016,102,156.
[12] A. Saylroy, S. Eiamsa-ard, Periodically fully-developed heat and fluid flow behaviors in a turbulent tube flow with square-cut twisted tape inserts, Applied Thermal Engineering 2017,112,895.
[13] S. W. Chang, T. L. Yang, J. S. Liou, Heat transfer and pressure drop in tube with broken twisted tape insert, Experimental Thermal and Fluid Science 2007,32,489.
[14] A. R. Abu Talib, A. K. Hilo, Fluid flow and heat transfer over corrugated backward facing step channel, Case Studies in Thermal Engineering, 2021,24,100862.
[15] J.S. Marcelo, de Lemos, M. Assato, Turbulence structure and heat transfer in a sudden expansion with a porous insert using linear and non-linear turbulence models, *International Journal of Thermal Sciences*, 2019,141,1.
[16] A. E. Zohir, A. G. Gomaa, Heat transfer enhancement through sudden expansion pipe airflow using swirl generator with different angles, Experimental Thermal and Fluid Science, 2013,45,146.
[17] K. S. Mushatet, Q. A. Rishakb, M. H. Fagr, Numerical study of laminar flow in a sudden expansion obstacled channel, *Journal of Thermal Science* 2015,19(2)657.
[18] V. I. Terekhov, M. A. Pakhomov, Predictions of turbulent flow and heat transfer in gas–droplets flow downstream of a sudden pipe expansion, *International Journal of Heat and Mass Transfer*, 2009,52,21,4711.
[19] R. R. Bilawane, N. K. Mandavgade, V. N. Kalbande, L. J. Patle, M. T. Kanojiya, R. D. Khorgade, Experimental investigation of natural convection heat transfer coefficient for roughed inclined plate, Materialstoday: Proceedings 2021.
[20] M. Attalla, H. M. Maghrabie, Investigation of effectiveness and pumping power of plate heat exchanger with rough surface, Chemical Engineering Science, 2020,211,115277.
[21] K. Nilpueng, S. Wongwises, Experimental study of single-phase heat transfer and pressure drop inside a plate heat exchanger with a rough surface, Experimental Thermal and Fluid Science 2015,68,268.
[22] M. Farnam, M. Khoshvaght-Aliabadi, M. J. Asadollahzadeh, Intensified single-phase forced convective heat transfer with helical-twisted tube in coil heat exchangers, Annals of Nuclear Energy, 2021,154,108108.
[23] C. Luo, K. Song, Thermal performance enhancement of a double-tube heat exchanger with novel twisted annulus formed by counter-twisted oval tubes, *International Journal of Thermal Sciences*, 2021,164,106892.
[24] C. Yu, H. Zhang, M. Zeng, B. Gao, Numerical study on turbulent heat transfer performance of twisted oval tube with different cross sectioned wire coil, Case Studies in Thermal Engineering, 2020,22,100759.
[25] X. Dong, X. Jin, P. Li, Q. Bi, M. Gui, T. Wang, Experimental research on heat transfer and flow resistance properties in spiral twisted tube heat exchanger, Applied Thermal Engineering, 2020,176,115397.
[26] J. P. Meyer, S. M. Abolarin, Heat transfer and pressure drop in the transitional flow regime for a smooth circular tube with twisted tape inserts and a square-edged inlet, *International Journal of Heat and Mass Transfer*, 2018,117,11.
[27] M. H. Fagr, H. M. Hasan, Z. M.A. Alsulaiei, Effects of helical obstacle on heat transfer and flow in a tube, Progress in Nuclear Energy 2021,137,103735.
[28] Lawrence B. Evans, The effect of axial turbulence promoters on heat transfer and pressure drop inside a tube, PhD thesis, University of Michigan, department of chemical and metallurgical engineering, IP 570, June, 1962.
[29] K. L. Kumar, Engineering Fluid Mechanics, Seventh Edition, ISBN: 81-219-0100-6.
[30] F. P. Incropera, D. P. DeWitt, Introduction to heat transfer, Fourth Edition, ISBN:0-471-38649-9.
[31] R.L. Webb, Performance evaluation criteria for use of enhanced heat transfer surfaces in heat exchanger design, Int. J. Heat Mass Transfer 1981,24,715.
[32] C. Zhang, D. Wang, K. Ren, Y. Han, Y. Zhu, X. Peng, J. Deng, X. Zhang, A comparative review of self-rotating and stationary twisted tape inserts in heat exchanger, Renewable and Sustainable Energy Reviews 2016,53,433.
[33] B. S. Petukhov, Heat Transfer and Friction in Turbulent Pipe Flow with Variable Physical Properties, Advances in Heat Transfer 1970,6,503.